

Supplementary Information

Kinetics and mechanisms of Cr(VI) Removal by nZVI: Influencing parameters and modification

Submitted to

Catalysts

Yizan Gao, Xiaodan Yang, Xinwei Lu, Minrui Li*, Lijun Wang, Yuru Wang*

Department of Environmental Science, School of Geography and Tourism, Shaanxi
Normal University, Xi'an 710119, China

* Corresponding author: Tel.: 15891779702 (Y.W.); 029-85310524 (M.L.)

E-mail address: liminrui@snnu.edu.cn (M.L.); wangyuru@snnu.cn (Y.W.)

Summary of contents:

Text S1;

Tables S1–S5;

Figures S1–S5

Text S1.

1. The reduction rates of nZVI for Cr(VI) reduction were obtained by following formula [1]:

$$\text{Cr removal efficiency (\%)} = \frac{C_0 - C_t}{C_0} \times 100\%$$

C_0 : is the initial Cr(VI) concentration in the solution;

C_t : the concentration of Cr(VI)in the solution at min.

2. The kinetic equation for the removal of Cr (VI) by nZVI was as follows:

first-order [2]: $\ln C = k_1 t + C_0$

second-order [3]: $1/C = k_2 t + C_1$

pseudo-first-order [4]: $\ln(q_e - q_t) = k_3 t + C_2$

pseudo-second-order [5]: $t/q_t = k_4 t + C_3$

C : the concentration of Cr(VI)in the solution at min.

3. The Langmuir and Freundlich isotherm models can be represented as follows:

Langmuir [6]: $q = kc^{1/n}$

Freundlich [7]: $q = q_e * bc / (1+bc)$

q : adsorption capacity at different time($\text{mg} \cdot \text{g}^{-1}$)

4. Intraparticle [8]: $q_t = k * t^{0.5} + C$

5. Formula for calculating adsorption capacity[9]: $q = \frac{v(c_0 - c)}{m}$

q : Adsorption capacity at adsorption equilibrium, mg/g ;

V : Solution volume, L ;

C_0 :Initial concentration of solution, mg/L ;

C : The concentration of solution at adsorption equilibrium at min, mg/L ;

Q_t : adsorption capacity of solution at adsorption equilibrium at min , mg/g ;

Q_e : maximum adsorption capacity, mg/g .

Table S1. The EDS results of pre- and post-reaction of Cr(VI) with nZVI.

| | Element | unn. C [wt.%] | norm. C [wt.%] | Atom. C [at.%] | Error (3 Sigma) [wt.%] |
|---------------|----------|------------------|-------------------|-------------------|---------------------------|
| pre-reaction | Iron | 74.01 | 95.16 | 84.92 | 6.03 |
| | Oxygen | 3.77 | 4.84 | 15.08 | 2.10 |
| | Gold | 0.00 | 0.00 | 0.00 | 0.00 |
| | Total: | 77.78 | 100.00 | 100.00 | |
| post-reaction | Iron | 69.72 | 70.93 | 42.04 | 5.67 |
| | Oxygen | 27.07 | 27.54 | 56.99 | 10.20 |
| | Chromium | 1.50 | 1.53 | 0.97 | 0.23 |
| | Gold | 0.00 | 0.00 | 0.00 | 0.00 |
| | Total: | 98.29 | 100.00 | 100.00 | |

Table S2. Comparison of R^2 values fitted by various kinetic models at different temperatures.

| | First order | Second order | Pseudo-first order | Pseudo-second order |
|------|------------------------------|-------------------------|--|--------------------------|
| 293K | $\text{LnC} = 0.031t + 2.93$ | $1/C = 0.0001t + 0.054$ | $\text{Ln}(Q_e - Q_t) = 0.0195t + 2.85$ | $t/Q_t = 0.019t + 0.075$ |
| | $R^2 = 0.7075$ | $R^2 = 0.6673$ | $R^2 = 0.8123$ | $R^2 = 0.9998$ |
| 303K | $\text{LnC} = 0.0109t +$ | $1/C = -0.0002t +$ | $\text{Ln}(Q_e - Q_t) = 0.0361t +$ | $t/Q_t = 0.01972t +$ |
| | 2.29 | 0.053 | 0.068 | 0.049 |
| 313K | $R^2 = 0.2352$ | $R^2 = 0.5492$ | $R^2 = 0.6822$ | $R^2 = 0.9997$ |
| | $\text{LnC} = 0.0033t +$ | $1/C = -9E-0.5t +$ | $\text{Ln}(Q_e - Q_t) = -0.0407t + 3.63$ | $t/Q_t = 0.019t + 0.097$ |
| | 2.89 | 0.050 | $R^2 = 0.8307$ | $R^2 = 0.9983$ |
| | $R^2 = 0.6809$ | $R^2 = 0.9122$ | | |

Table S3. Comparison of R^2 values fitted by isothermal adsorption model.

| T (K) | Langmuir | | | Freundlich | | |
|-------|--------------|--------------|--------|------------|-------|--------|
| | Q_m (mg/g) | K_L (L/mg) | R^2 | n/1 | K_F | R^2 |
| 293 | 57.077 | 1.46 | 0.9719 | 0.4329 | 25.11 | 0.9017 |

Table S4. Intraparticle diffusion coefficients and intercept values for Cr(VI)

adsorption on nZVI particles at different temperatures.

| Step.1 | | | |
|-----------------|--|----------------------|----------------|
| Temperature (K) | K ($\text{mg}\cdot\text{g}^{-1}\cdot\text{h}^{0.5}$) | Intercept values (C) | R ² |
| 293 K | 10.67 | 2.62 | 0.92 |
| 303 K | 11.48 | 2.25 | 0.93 |
| 313 K | 10.98 | 1.75 | 0.95 |

| Step.2 | | | |
|-----------------|--|----------------------|----------------|
| Temperature (K) | K ($\text{mg}\cdot\text{g}^{-1}\cdot\text{h}^{0.5}$) | Intercept values (C) | R ² |
| 293 K | 37.82 | 1.39 | 1 |
| 303 K | 41.49 | 0.98 | 1 |
| 313 K | 32.85 | 1.71 | 1 |

| Step.3 | | | |
|-----------------|--|----------------------|----------------|
| Temperature (K) | K ($\text{mg}\cdot\text{g}^{-1}\cdot\text{h}^{0.5}$) | Intercept values (C) | R ² |
| 293 K | 50 | -8.95E-15 | 1 |
| 303 K | 45.38 | 0.207 | 1 |
| 313 K | 47.26 | 0.441 | 1 |

Table S5. Comparison of the Cr(VI) removal efficiency of nZVI and other related materials

| Sorbent | pH | Adsorption rate (mg/g/h) | Adsorption capacity (mg/g) |
|---|-----|-----------------------------|----------------------------|
| nano-magnetite[10] | 6.0 | 3.7 | 1.5 |
| Fe ₃ O ₄ @poly(m-phenylenediamine) particle[11] | 2.0 | 49.2 | 246.0 |
| Magnetite[12] | 2.0 | 7.5 | 12.5 |
| liquid nitrogen treated zero-valent iron[13] | 6.3 | 0.4 | 0.4 |
| graphene oxide hydrogel with shrimp shell magnetic biochar[14] | 1.0 | 28.6 | 85.9 |
| ball milling synthesized FeS ₂ @biochar composite[15] | 3.0 | 57.5 | 134.0 |
| nZVI | 3.0 | 25.0 | 50.0 |
| H ₂ A-nZVI | 3.0 | 66.7 | 50.0 |
| Starch-nZVI | 3.0 | 200.0 | 50.0 |
| Fe-Cu | 3.0 | 100.0 | 50.0 |

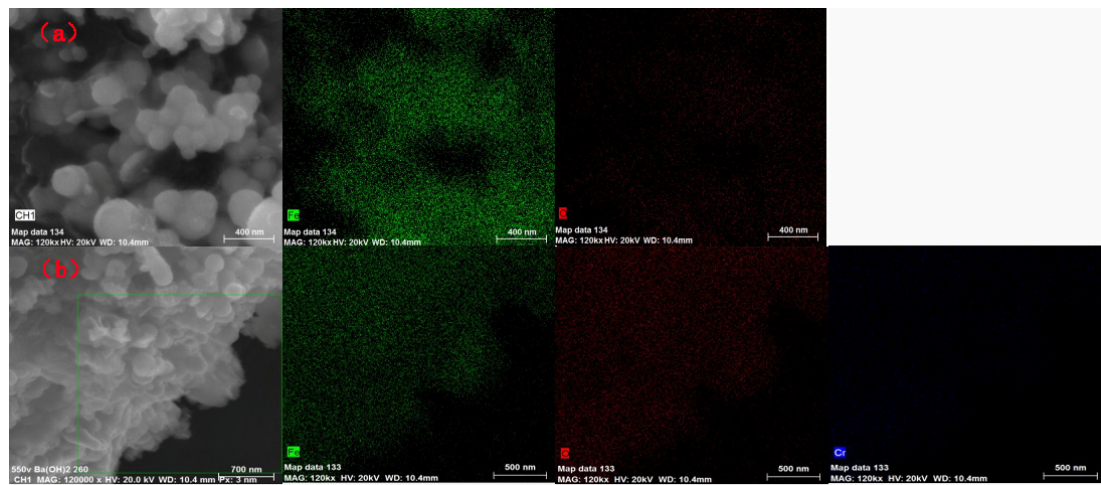


Figure S1. The EDS results of pre- (a) and post- (b) reaction of Cr(VI) with nZVI.

($[Cr(VI)] = 25 \text{ mg/L}$, $[nZVI] = 0.5 \text{ g/L}$, $pH = 3$, $T = 293 \text{ K}$)

It can be seen from the Figure S1 that the content of Fe before the reaction is obviously higher than that after the reaction, while the content of O before the reaction is obviously lower than that after the reaction, which further proves that O participates in the removal of Cr(VI).

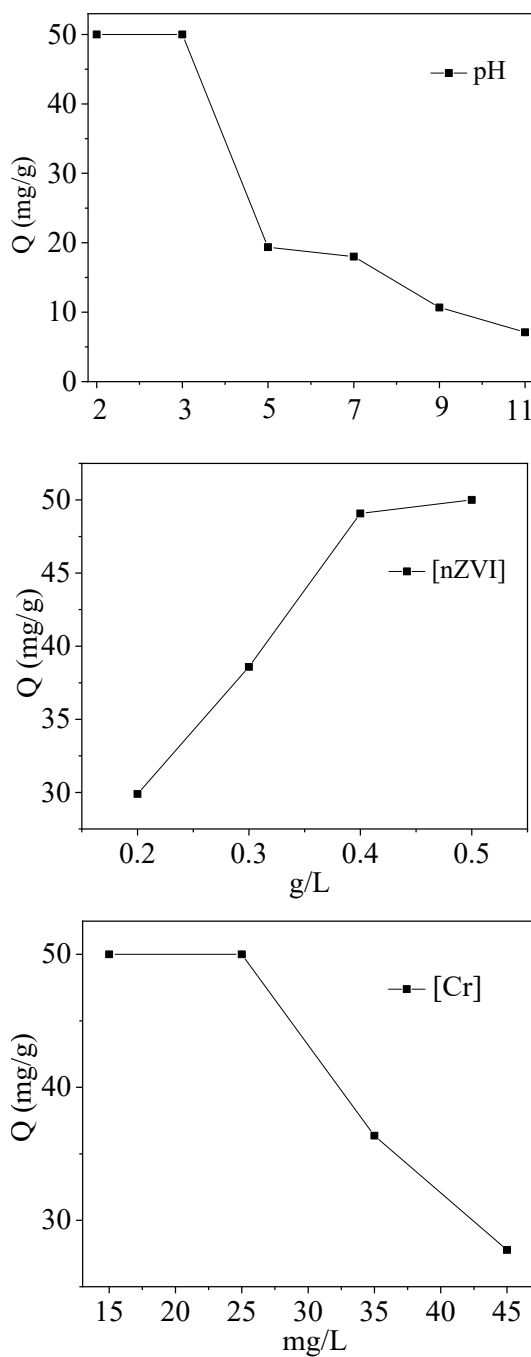


Figure S2. Changes of adsorption capacity with pH, initial concentration of Cr(VI) and dosage of nZVI.

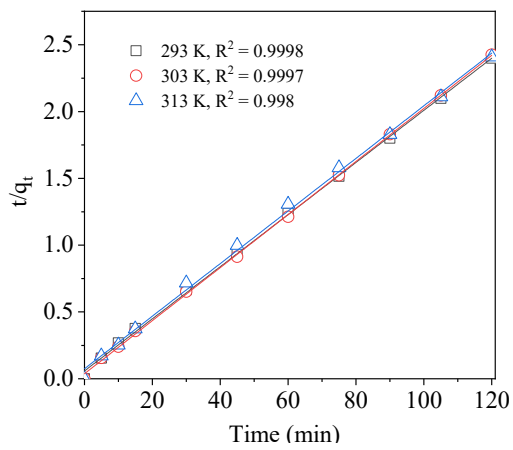


Figure S3. Pseudo-second-order kinetic fitting curve of Cr(VI) removal by nZVI.

([Cr(VI)] = 25 mg/L, [nZVI] = 0.5 g/L, pH = 3, T = 120 min)

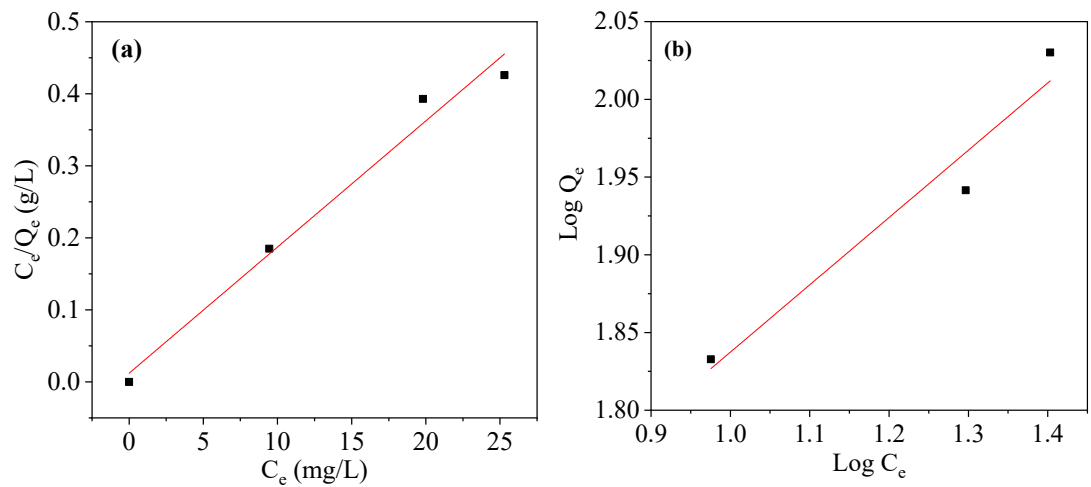


Figure S4. Fitting results of isotherm adsorption model (a: Langmuir; b: Freundlich).

([nZVI] = 0.5 g/L, pH = 3, T = 293 K)

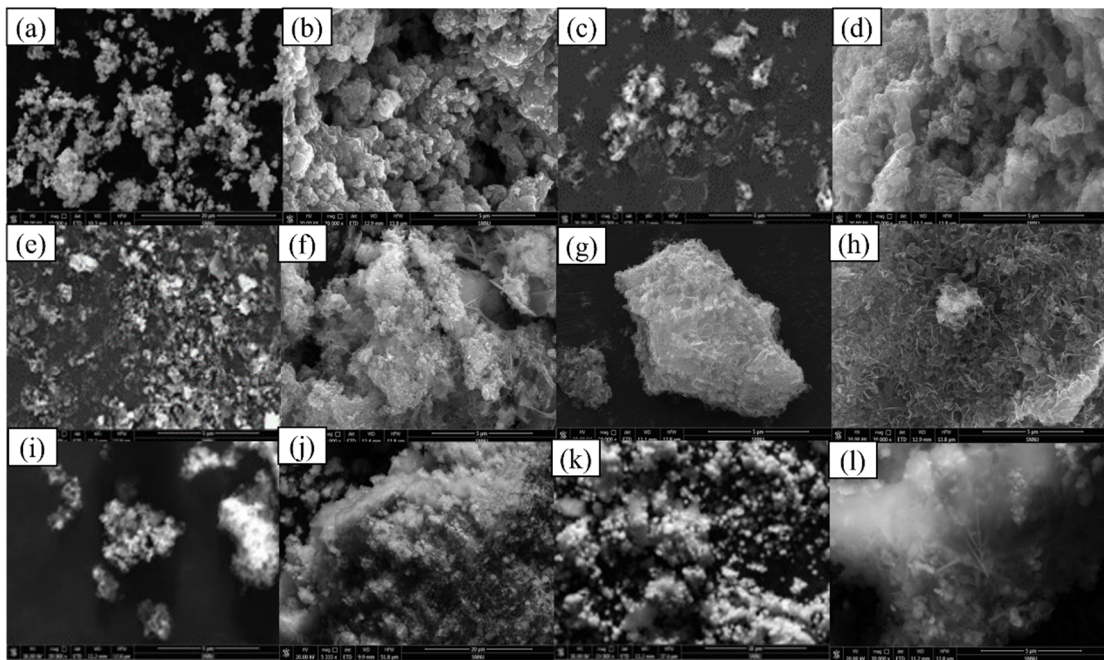


Figure S5. The SEM results of pre- and post- reaction of Cr(VI) with supported nZVI [(a,b) H₂A-nZVI; (c,d) Starch-nZVI; (e,f) Fe-Cu; (g,h) CMC-nZVI; (i,j) Fe-Zn; (k,l) Fe-Mn].

([Cr(VI)] = 25 mg/L, [nZVI] = 0.5 g/L, pH = 3, T = 293 K)

References

1. Xu, Y.; Chen, J.; Chen, R.; Yu, P.; Guo, S.; Wang, X., Adsorption and reduction of chromium(VI) from aqueous solution using polypyrrole/calcium rectorite composite adsorbent. *Water Research* 2019, 160, 148-157.
2. Sadeq, Y.; Poulsen, T. G.; Bester, K., Modeling organic micro pollutant degradation kinetics during sewage sludge composting. *Waste Management* 2014, 34 (11), 2007-2013.
3. Ho, Y.-S., Review of second-order models for adsorption systems. *Journal of Hazardous Materials* 2006, 136 (3), 681-689.
4. Feng, J.; Su, L.; Ma, Y.; Ren, C.; Guo, Q.; Chen, X., CuFe₂O₄ magnetic nanoparticles: A simple and efficient catalyst for the reduction of nitrophenol. *Chemical Engineering Journal* 2013, 221, 16-24.
5. Ho, Y. S.; Ng, J. C. Y.; McKay, G., Kinetics of pollutant sorption by biosorbents: Review. *Separation and Purification Methods* 2000, 29 (2), 189-232.
6. Foo, K. Y.; Hameed, B. H., Insights into the modeling of adsorption isotherm systems. *Chemical Engineering Journal* 2010, 156 (1), 2-10.
7. Al-Ghouti, M. A.; Da'ana, D. A., Guidelines for the use and interpretation of adsorption isotherm models: A review. *Journal of Hazardous Materials* 2020, 393.
8. Kegl, T.; Kosak, A.; Lobnik, A.; Novak, Z.; Kralj, A. K.; Ban, I., Adsorption of rare earth metals from wastewater by nanomaterials: A review. *Journal of Hazardous Materials* 2020, 386.
9. Zhao, J.; Boada, R.; Cibin, G.; Palet, C., Enhancement of selective adsorption of Cr species via modification of pine biomass. *Science of the Total Environment* 2021, 756.
10. Komarek, M.; Koretsky, C. M.; Stephen, K. J.; Alessi, D. S.; Chrastny, V., Competitive Adsorption of Cd(II), Cr(VI), and Pb(II) onto Nanomagheme: A Spectroscopic and Modeling Approach. *Environmental Science & Technology* 2015, 49 (21), 12851-12859.
11. Wang, T.; Zhang, L.; Li, C.; Yang, W.; Song, T.; Tang, C.; Meng, Y.; Dai, S.; Wang, H.; Chai, L.; Luo, J., Synthesis of Core-Shell Magnetic Fe₃O₄@poly(m-Phenylenediamine) Particles for Chromium Reduction and Adsorption. *Environmental Science & Technology* 2015, 49 (9), 5654-5662.

12. Ben Tahar, L.; Oueslati, M. H.; Abualreish, M. J. A., Synthesis of magnetite derivatives nanoparticles and their application for the removal of chromium (VI) from aqueous solutions. *Journal of Colloid and Interface Science* 2018, 512, 115-126.
13. Hu, Y.; Peng, X.; Ai, Z.; Jia, F.; Zhang, L., Liquid Nitrogen Activation of Zero-Valent Iron and Its Enhanced Cr(VI) Removal Performance. *Environmental Science & Technology* 2019, 53 (14), 8333-8341.
14. Mahmoud, M. E.; Mohamed, A. K.; Salam, M. A., Self-decoration of N-doped graphene oxide 3-D hydrogel onto magnetic shrimp shell biochar for enhanced removal of hexavalent chromium. *Journal of Hazardous Materials* 2021, 408.
15. Tang, J.; Zhao, B.; Lyu, H.; Li, D., Development of a novel pyrite/biochar composite (BM-FeS₂@BC) by ball milling for aqueous Cr(VI) removal and its mechanisms. *Journal of Hazardous Materials* 2021, 413.